Int. J. Multiphase Flow Vol. 19, No. 3, pp. 509–525, 1993
Printed in Great Britain

0301-9322/93 $6.00 + 0.00
Pergamon Press Ltd

HISTORY FORCE ON A SPHERE DUE TO A STEP CHANGE IN THE FREE-STREAM VELOCITY

R. MEI

Department of Aerospace Engineering, Mechanics & Engineering Science, University of Florida, Gainesville, FL 32611, U.S.A.

(Received 29 April 1992; in revised form 27 December 1992)

Abstract—Finite-difference solutions for unsteady flows over a stationary sphere due to a step change in the free-stream velocity from U_1 to U_2 ($0 \leqslant U_1 < U_2$) are obtained, from which the unsteady drag is evaluated, for Reynolds numbers, Re (based on the diameter of the sphere and the free-stream velocity U_2), ranging from 0.1 to 100 over a large range of time. The history force on the sphere is determined by subtracting the quasi-steady drag from the computed total drag. The numerical result shows a complicated behavior of the history force at finite Re for both $U_1 = 0$ and $U_1 > 0$. It decays as $t^{-1/2}$ for small time; it then decays as t^{-n} ($n \geqslant 2$ with $n = 2$ for small Re) for an intermediate range of time; and it decays exponentially at large time. The numerical results are used to assess a recently developed expression for the history force for finite Re. Good overall agreement is observed for the history force between the analytical prediction and the finite-difference solution for small and intermediate time for the Re values tested.

Key Words: particle dynamics, history force, finite Reynolds number

1. INTRODUCTION

In order to predict unsteady motions of particles (including droplets and bubbles) in a carrier fluid, a precise knowledge of the unsteady forces on the particles is required. In steady state, the drag on a particle due to the fluid flow is mainly dependent on the Reynolds number, Re, which is based on the relative velocity and the particle diameter. In many situations, significant variations in the velocities of both the fluid and particles are encountered, such as particles suspended in a high-speed mixing layer where large spatial velocity gradients exist, high-pressure spray injection of liquid fuel in combustors, among others. The acceleration of the relative flow thus introduces an additional complexity, especially at finite Re, to the dynamics describing the particle motion and it needs to be properly taken into account.

The earliest works related to the unsteady drag on a spherical particle were those of Stokes (1851) and Basset (1888). Their results were derived in the frequency and time domains, respectively, in the creeping flow regime for zero Re. Odar & Hamilton (1964) performed carefully controlled experiments to measure the unsteady drag on an oscillating sphere in a stagnant oil tank for $\mathrm{Re} < 62$. Modifications on the history force and the added-mass force were proposed based on an acceleration parameter (Odar 1966). Their empirical result has been used, for example: by Schöneborn (1975) to correlate his experimental results for the reduction of the particle settling velocity in an oscillating flow field; by Clift *et al.* (1978) to predict the motion of a falling sphere in a stagnant liquid pool with large Re based on the terminal velocity; and by Linteris *et al.* (1991) to study the droplet dynamics in a nonuniform flow field. Temkin and coworkers (Temkin & Kim 1980; Temkin & Mehta 1982) deduced a drag coefficient as a function of Re and flow acceleration from accurate photographic measurements of droplet trajectories induced by weak shock waves in a horizontal shock tube. It was found that when the flow relative to the droplet is accelerating (decelerating), the drag coefficient is smaller (larger) than the steady-state value at the same velocity. This trend directly contradicts the prediction given by the solutions of Stokes and Basset and the experimental results of Odar & Hamilton (1964), Schöneborn (1975) and Karanfillian & Kotas (1978) regarding the effect of flow acceleration on the unsteady drag. Recently, Tsuji *et al.* (1991) measured the unsteady drag on a sphere due to a finite fluctuation of the free-stream velocity at high Re (~8000–16,000). The results clearly show that the instantaneous unsteady drag should be larger than the corresponding steady-state value at the same velocity when the flow accelerates.

Recently, Mei and coworkers (Mei 1990, 1993; Mei *et al.* 1991; Mei & Adrian 1992) showed, through detailed theoretical and numerical analyses, that the force on a sphere in an unsteady flow field consists of a quasi-steady drag, a history force, an added-mass force and a force associated with the free-stream acceleration for $\mathrm{Re} \leqslant 200$. At finite Re, the quasi-steady drag can be represented by using the standard steady-state drag coefficient and the instantaneous velocity; the added-mass force is the same as in the creeping flow and potential flow regimes; the history force has a kernel that decays as $t^{-1/2}$ for small time and as t^{-2} for large time. An approximation for the history-force kernel was derived for finite Re (Mei & Adrian 1992). In Mei (1993), the analytical prediction of the total unsteady drag on an oscillating sphere in a stagnant oil tank based on this approximation was shown to be in fair agreement with the experimental results of Odar & Hamilton (1964) at finite frequencies. The predicted velocity for a falling sphere in a stagnant liquid pool was in very close agreement with the experimentally measured values over a large range of Re (Moorman 1955). The particle dynamic equation proposed in Mei & Adrian (1992) agrees in principle with the experimental results of Odar & Hamilton (1964) and Tsuji *et al.* (1991) and approaches Basset's (1888) solution for the unsteady drag in the limit as $t \to 0$ for small Re. For an oscillating sphere at finite Re (Mei 1993), the quasi-steady force is shown to be the dominant term in the total drag and its representation using the steady drag coefficient and instantaneous velocity is accurate at low frequency. At high frequency, the quasi-steady force based on the steady drag coefficient results in an $O(1)$ error (an overestimation) in comparison with an asymptotic solution. However, this error is very small in comparison with the leading order terms (added-mass and history forces) in the total drag at high frequency. Mei (1993) also pointed out that the modifications on the history force and added-mass force by Odar & Hamilton (1964) were not physically sound, because they do not give correct long-time asymptotic decay of the history force and do not approach Stokes's (1851) solution as $\mathrm{Re} \to 0$. Their expressions for the history force and added-mass force both exhibit unphysical behavior at some particular instant in a purely oscillating flow, but tend to cancel each other in the expression for the total unsteady drag for the oscillating flow. They do not approach the limiting behavior of Basset's (1888) solution at small time. In summary, the carefully controlled experimental results of Odar & Hamilton (1964), Schöneborn (1975) and Tsuji *et al.* (1991) at finite Re agree qualitatively with the classical theories of Stokes (1851) and Basset (1888) for zero Re and the recently developed theory of Mei & Adrian (1992) for finite Re, while the carefully obtained experimental results of Temkin & Kim (1980) and Temkin & Mehta (1982) showed the opposite trend. Because of the particular setup using a shock tube in the experimental investigations by Temkin & Kim (1980) and Temkin & Mehta (1982), it appears that the particle dynamics involving a sudden change in the free-stream velocity must be understood first at finite Re.

For the impulsively started motion, $U_1 = 0$, an analytical solution for the unsteady drag has been obtained by Sano (1981) for $\mathrm{Re} \ll 1$ using the method of matched asymptotic expansions. The unsteady drag was found to approach to the steady value as t^{-2} at long time. However, the result is for very low Re, strictly speaking. In this study, the unsteady flow has a zero acceleration at $t > 0$. The difference between the steady drag and unsteady drag will be taken as the history force. As just mentioned, there is some error in representing the quasi-steady drag by the steady drag at high frequency or small time. However, the variation in the flow field at long time is very small, so the quasi-steady force is accurately represented by the steady drag. Thus, the long-time history force can be accurately computed, while the short-time history force has an $O(1)$ error; which is rather small in comparison with $O(t^{-1/2})$. It is not clear if the history force to be computed for this particular unsteady flow should decay as t^{-2} or not at long time for finite Re.

In Mei & Adrian (1992), an unsteady flow over a stationary sphere due to a small oscillation in the free-stream velocity, $\alpha U\, \mathrm{e}^{-i\omega t'}$ ($\alpha \ll 1$), was investigated. An expression for the history force that leads to a t^{-2} decay at large time was given (see [7a, b]). However, the results were derived from an interpolation in the frequency domain based on the asymptotic limits of the history force at low and high frequencies:

$$D_{11\mathrm{H}}(\mathrm{St}) \approx \frac{-f_{\mathrm{H}}(\mathrm{Re}')\mathrm{St}}{\left\{1 + \left[\dfrac{2f_{\mathrm{H}}^2(\mathrm{Re}')\mathrm{St}}{\mathrm{Re}'}\right]^{m/2}\right\}^{1/m}}, \quad m = 2, \tag{1}$$

in which $St = \omega a/U$ is the Strouhal number, $Re' = Re/2$, f_H is given by [7b] and D_{11H} is the imaginary component of the history force coefficient in the frequency domain [see Mei & Adrian (1992) for details]. In the low-frequency end, it was only established that the history force is proportional to the frequency, $D_{11H}(St) \sim f_H(Re')St$ as $St \to 0$, through numerical computation (Mei *et al.* 1991) and asymptotic analysis (Mei & Adrian 1992). If a different form of interpolation for the history force was used, e.g. by choosing $m \neq 2$ in [1], but with the same low- and high-frequency asymptotic limits, one would get, through numerical integration, a history force with a long-time decay in the form of t^{-n} in which n may not necessarily be equal to 2 at finite Re. The determination of the long-time behavior of the history force thus requires a precise knowledge of the history force in the frequency domain, which is very difficult to obtain accurately.

Because of the particular nature of the acceleration of the flows with a step change in the free-stream velocity from U_1 to U_2 ($0 \leqslant U_1 < U_2$), the history force can be determined in the time domain through careful computations using a finite-difference method. The result allows for an examination of the exact (except for the truncation error and machine error) long-time behavior of the history force and for an assessment of the particle dynamic equation proposed by Mei & Adrian (1992) in the case of zero acceleration following an impulsive acceleration in the free-stream velocity. In this paper, finite-difference solutions for the unsteady flow field are obtained for Re, based on the diameter of the sphere, ranging from 0.1 to 100. Two cases are considered: (i) $U_1 = 0$; and (ii) $U_1 > 0$. For the impulsively started flow, $U_1 = 0$, the initial field is vorticity free, while for $U_1 > 0$ there already exists a steady vorticity field at finite Re. The long-time behavior of the history force may be influenced by the structure of the steady vorticity and the comparison between these two cases shall show if such effects are important or not. It is found that the existing steady vorticity has no significant effect on the qualitative behavior of the long-time history force. The history force decays as $t^{-1/2}$ for small time, say $t < 1$; it decays as t^{-n} ($n \geqslant 2$) in the intermediate range of time, say $t \sim 10$; and it finally decays exponentially at very large time, say $t > 100$, in which t is made dimensionless by U_2 and the radius of the sphere. Good overall agreement between the analytical prediction using the expression of Mei & Adrian (1992) and the present numerical result is achieved for small and intermediate time.

2. ANALYSIS

2.1. Particle Dynamic Equation at Finite Re

For a stationary sphere experiencing a small fluctuation $u_1'(t')$ in the free-stream velocity U' with $|u_1'(t')| \ll U'$, Mei & Adrian (1992) obtained the following expression for the total unsteady drag at finite Re:

$$F'(t') = F'_{QS}(t') + F'_H(t') + F'_{AM}(t') + F'_{FS}(t'), \qquad [2]$$

where F'_{QS} is the quasi-steady drag as if the acceleration of the flow is vanishingly small, F'_H is the history force (or the memory force), F'_{AM} is the added-mass force and F'_{FS} is due to the unsteadiness and the spatial nonuniformity of the free-stream velocity. If the sphere oscillates while the free stream is steady and uniform, $F'_{FS}(t') = 0$. In this paper, the prime denotes dimensional quantities unless otherwise mentioned. These forces are given, respectively, as

$$F'_{QS}(t') = 6\pi\mu a U'(t')\phi(Re), \qquad [3]$$

$$F'_H(t') = 6\pi\mu a \int_{-\infty}^{t'} K(t'-\tau)\frac{dU'}{d\tau}\,d\tau, \qquad [4]$$

$$F'_{AM}(t') = \tfrac{2}{3}\rho_f \pi a^3 \frac{dU'}{dt'} \qquad [5]$$

and

$$F'_{FS}(t') = \tfrac{4}{3}\rho_f \pi a_3 \frac{DU'}{Dt'}, \qquad [6]$$

with the history-force kernel being

$$K(t'-\tau) \approx \left\{\left[\frac{\pi(t'-\tau)\nu}{a^2}\right]^{1/4} + \left[\frac{\pi}{2}\frac{U'^3}{a\nu f_H^3(\mathrm{Re})}(t'-\tau)^2\right]^{1/2}\right\}^{-2} \qquad [7a]$$

and

$$f_H(\mathrm{Re}) = 0.75 + 0.105\mathrm{Re}, \quad \mathrm{Re} = \frac{2aU'}{\nu}, \qquad [7b]$$

where μ and ν are the dynamic and kinematic viscosities of the fluid, ρ_f is the fluid density and a is the radius of the sphere. The factor $\phi(\mathrm{Re})$ accounts for the deviation from the Stokesian drag for $\mathrm{Re}(t') > 0$. Many forms of $\phi(\mathrm{Re})$ at different ranges of Re can be found in Clift *et al.* (1978) and the following forms are considered accurate for practical purposes:

$$\begin{aligned}
\phi &= 1 + \frac{3}{16}\mathrm{Re}, && \mathrm{Re} \leqslant 0.01,\\
&= 1 + 0.1315\mathrm{Re}^{0.82 - 0.05w}, && 0.01 < \mathrm{Re} \leqslant 20,\\
&= 1 + 0.1935\mathrm{Re}^{0.6305}, && 20 < \mathrm{Re} \leqslant 260,
\end{aligned} \qquad [8]$$

with $w = \log_{10}\mathrm{Re}$. In [8], Re takes the instantaneous value.

The expression for the history-force kernel given by [7a] for an unsteady flow over a stationary sphere was based on: (i) the numerical result of the small-amplitude free-stream oscillation at finite Re for a wide range of frequencies; (ii) the asymptotic result of the small-amplitude oscillation case at small Re and low frequency, which gives the long-time behavior of the kernel $K(t'-\tau)$; (iii) the Stokes solution for high-frequency oscillation; and (iv) the principle of causality, i.e. the motion of the particle can be influenced only by its previous history, not by its future behavior. The important feature of this modified history-force kernel is that it decays as $(t'-\tau)^{-2}$ at large time as opposed to $(t'-\tau)^{-1/2}$ as derived by Basset (1888). This implies a much more rapid decay of the initial condition or disturbance on the particle motion in an unsteady flow.

Although the theory was developed for both small and finite Re, the accelerations of these unsteady flows investigated by Mei and coworkers (Mei *et al.* 1991; Mei & Adrian 1992; Mei 1993) were nevertheless quite well-behaved in comparison with that involving a shock wave as investigated by Temkin & Kim (1980) and Temkin & Mehta (1982). In addition, the added-mass force was deduced based on the asymptotic behavior of the high-frequency oscillation; the history force was determined by subtracting the added-mass force from the total imaginary component of the unsteady force in the frequency domain (see Mei 1990; Mei *et al.* 1991; Mei 1993). The correctness of the low-frequency behavior of the history force was thus based on the assumption that the added-mass at low frequency is the same as that at high frequency. Although this assumption was confirmed by Rivero *et al.* (1991) for an oscillating flow and a constantly accelerating flow over a sphere, by carrying out an ingenious numerical procedure to separate the contributions to the total unsteady force from the history force and the instantaneous added-mass force, it is not tested for other types of flows yet.

It is commonly viewed that the added-mass force is a force related to the instantaneous acceleration. For an unsteady flow over a stationary sphere due to a sudden change, from U_1 to U_2 $(0 \leqslant U_1 < U_2)$, in the free-stream velocity, the acceleration is zero at $t' > 0$, which results in a zero added-mass force for $t' > 0$. Since the quasi-steady force can be determined from the steady drag corresponding to U_2, this special unsteady flow thus allows for a complete separation of the history force from the added-mass force and the quasi-steady force. It also represents a *severe test case* for the history force expression given by [7a, b] because the acceleration function is strongly singular, while in previous studies it was rather well-behaved.

For a step change in the free-stream velocity, the evaluation of the history force is not trivial. Let $\Delta U = U_2 - U_1$ be the velocity change, say due to a weak shock wave produced in a shock tube (Temkin & Kim 1980; Temkin & Mehta 1982), the acceleration is $\mathrm{d}U'/\mathrm{d}t' = \Delta U\delta(t')$, with $\delta(t')$

being the Dirac delta function defined as $\delta(t') = 0$ for $t' \neq 0$ and $\int_{0^-}^{0^+} \delta(t')\,dt' = 1$. From [5] and [6] the forces related to the instantaneous acceleration are

$$F'_{AM}(t') = \tfrac{2}{3}\rho_f \pi a^3 \Delta U \delta(t') \qquad [9]$$

and

$$F'_{FS}(t') = \tfrac{4}{3}\rho_f \pi a^3 \Delta U \delta(t'). \qquad [10]$$

For $t' > 0$, the previous discussion leads to the following expressions for the quasi-steady force and the history force:

$$F'_{QS}(t') = 6\pi\mu a U_2 \phi(\mathrm{Re}) \qquad [11]$$

and

$$F'_H(t') = 6\pi\mu a \int_{0^-}^{t'} K(t' - \tau)\,\Delta U \delta(\tau)\,d\tau$$

$$= 6\pi\mu a\, \Delta U K(t'). \qquad [12]$$

The total drag on the sphere for $t' > 0$ in the above theoretical framework is thus

$$\frac{F'_T(t')}{6\pi\mu a U_2} = \phi(\mathrm{Re}) + \frac{\Delta U}{U_2} K(t'). \qquad [13a]$$

Since the total drag $F'_T(t')$ for $t' > 0$ can be obtained accurately by numerically solving the flow field around the sphere and integrating the stresses on the surface of the sphere, the history-force kernel $K(t')$ is determined from [13a] as

$$K(t') = \frac{U_2}{\Delta U}\left[\frac{F'_T(t')}{6\pi\mu a U_2} - \phi(\mathrm{Re})\right]. \qquad [13b]$$

The steady value $\phi(\mathrm{Re})$ in [13b] is obtained from

$$\phi(\mathrm{Re}) = \frac{F'_T(\infty)}{6\pi\mu a U_2}. \qquad [13c]$$

The numerical procedure for obtaining $F'_T(t')$ is outlined below.

2.2. Finite-difference Solution for the Unsteady Drag with a Step Change in the Free-stream Velocity

2.2.1. Governing equations, boundary and initial conditions

Using the stream function–vorticity, (ψ', ζ'), formulation, the unsteady Navier–Stokes equation for axisymmetric flow in spherical coordinates (r', θ) is

$$\frac{\partial}{\partial t'}(\zeta' r' \sin\theta) + \sin\theta\left[\frac{\partial}{\partial\theta}\left(\frac{\partial\psi'}{\partial r'}\frac{\zeta'}{r'\sin\theta}\right) - \frac{\partial}{\partial r'}\left(\frac{\partial\psi'}{\partial\theta}\frac{\zeta'}{r'\sin\theta}\right)\right] = \nu \mathscr{D}'^2(\zeta' r' \sin\theta) \qquad [14]$$

and

$$\mathscr{D}'^2\psi' = \zeta' r' \sin\theta, \qquad [15]$$

with

$$\mathscr{D}'^2 = \frac{\partial^2}{\partial r'^2} + \frac{\sin\theta}{r'^2}\frac{\partial}{\partial\theta}\left(\frac{1}{\sin\theta}\frac{\partial}{\partial\theta}\right). \qquad [16]$$

In the above, θ is measured from the front stagnation point. The boundary conditions for ψ' and ζ' at $t' > 0$ are

$$\psi' = \frac{\partial \psi'}{\partial r'} = 0 \qquad \text{on } r' = a, \tag{17}$$

$$\psi' = \zeta' = 0 \qquad \text{on } \theta = 0 \quad \text{and} \quad \pi \tag{18}$$

and

$$\psi' \to \tfrac{1}{2} U_2 r'^2 \sin^2\theta \quad \text{as } r' \to \infty. \tag{19}$$

Two slightly different flows with different initial conditions are considered. For the first case, $U_1 = 0$; and the initial conditions can be given explicitly as

$$\psi'(t', r', \theta) = \zeta'(t', r', \theta) = 0 \quad \text{at } t' = 0. \tag{20}$$

For the second case, $U_1 > 0$; the initial condition must be obtained by solving the steady flow field corresponding to $U = U_1$. Upon introducing the following dimensionless quantities,

$$r = r'/a, \quad t = t' U_2/a, \quad u = u'/U_2, \quad \psi = \psi'/(U_2 a^2), \quad \zeta = \zeta' a/U_2, \quad \mathscr{D}^2 = a^2 \mathscr{D}'^2, \tag{21}$$

and defining

$$y = r \sin\theta \tag{22}$$

and

$$g = \zeta y, \tag{23}$$

[14] and [15] become

$$\frac{\partial g}{\partial t} + \sin\theta \left[\frac{\partial}{\partial \theta}\left(\frac{\partial \psi}{\partial r}\frac{g}{y^2}\right) - \frac{\partial}{\partial r}\left(\frac{\partial \psi}{\partial \theta}\frac{g}{y^2}\right)\right] = \frac{2}{\mathrm{Re}} \mathscr{D}^2 g \tag{24}$$

and

$$\mathscr{D}^2 \psi = g; \tag{25}$$

the boundary conditions are

$$\psi = \frac{\partial \psi}{\partial r} = 0 \qquad \text{on} \quad r = 1, \tag{26}$$

$$\psi = g = 0 \qquad \text{on} \quad \theta = 0 \quad \text{and} \quad \pi \tag{27}$$

and

$$\psi \to \tfrac{1}{2} r^2 \sin^2\theta \quad \text{as} \quad r \to \infty. \tag{28}$$

In [24],

$$\mathrm{Re} = U_2 2a/\nu \tag{29}$$

is the Reynolds number based on the free-stream velocity at $t > 0$ and the diameter of the sphere.

For the impulsively started flow over a stationary sphere, $U_1 = 0$, an accurate solution for the stream function can be obtained at $t \ll 1$ by solving the unsteady Stokes equation, as given in Bentwich & Miloh (1978):

$$\begin{aligned} \psi(t, r, \theta) = \sin^2\theta \Bigg\{ & \tfrac{1}{2} r^2 - \frac{1}{2r}\left[1 + 3\left(\frac{4t}{\pi}\right)^{1/2} + 3t\right] \\ & + \tfrac{3}{2} t^{1/2}\left[\left(\frac{4}{\pi}\right)^{1/2} \exp(-\eta^2) - 2\eta \,\mathrm{erfc}(\eta)\right] \\ & + \frac{3}{2}\frac{t}{r}\left[(1 + 2\eta^2)\mathrm{erfc}(\eta) - \left(\frac{4}{\pi}\right)^{1/2} \eta \exp(-\eta^2)\right]\Bigg\}, \end{aligned} \tag{30}$$

where $\eta = (r-1)/(4t)^{1/2}$. From [30], the discrete values of $g(t, r, \theta)$ can be evaluated in a finite-difference form. Such solutions for $\psi(t, r, \theta)$ and $g(t, r, \theta)$ are used as the actual initial condition at, say, $t = 0.001$ (for accurate short-time solution) or 0.1 (for accurate long-time solution). Because the computation is carried out for $t > 0$, the forces associated with the instantaneous acceleration, $F_{AM}(t)$ and $F_{FS}(t)$, do not show up in the total unsteady drag. Thus, [30] is used rather than [20].

For the second case, the steady flow field at $\mathrm{Re}_1 = U_1 2a/\nu$ is first obtained. An increase in the dimensional free-stream velocity, which results in $\mathrm{Re} = U_2 2a/\nu$ based on the new free-stream velocity, is then specified at $t = 0$. After re-scaling the dependent and independent variables using the new free-stream velocity U_2, the initial value for the stream function, $\psi(t = 0, r, \theta; \mathrm{Re})$, remains the same as that given by the steady solution at $\mathrm{Re} = \mathrm{Re}_1$, $\psi(t \to \infty, r, \theta; \mathrm{Re}_1)$. The initial value for the vorticity-related function, $g(t = 0, r, \theta; \mathrm{Re})$, becomes $(U_1/U_2)g(t \to \infty, r, \theta; \mathrm{Re}_1)$ after rescaling by U_2.

2.2.2. Clustering of the grid and discretization of the equations

The numerical computation is performed in a physical domain of $1 \leqslant r \leqslant r_E$ and $0 \leqslant \theta \leqslant \pi$ using $N_\theta = 65$ or 129 grid points in the θ-direction and $N_r = 65$, 129 or 257 grid points in the r-direction. The following transformation is applied to place more grid points near the surface:

$$r = 1 + (r_E - 1)\{1 - c \tan^{-1}[(1 - x_2)\tan(1/c)]\}. \qquad [31]$$

Here, x_2 is the normal coordinate in the computational domain with $0 \leqslant x_2 \leqslant 1$.

The determination of r_E turns out to be a very subtle and important issue. One of our goals in this paper is to understand the long-time behavior of the history force. However, the history force is basically an accumulated effect (in the temporal direction) of the entire flow field. For small time, the rapid change in the vorticity field occurs near the sphere and the size of the physical domain r_E is not important. Since the dimensionless convection speed is one, the disturbance travels as $x \sim t$, while the additional distance due to the viscous diffusion is $x \sim (t/\mathrm{Re})^{1/2}$—which may be neglected for finite Re and large t. Due to the lack of knowledge of the effect of boundary conditions on the history force, we do not wish to see the disturbance reflected back from the boundary at $r = r_E$, which may affect the long-time behavior of the history force. It turns out that the long-time behavior of the history force is not clear until $t \sim 200$ to 300 for $\mathrm{Re} \leqslant 10$. Thus, a very large r_E is desirable. In this study, the history force at large time (beyond $t = 250$) for $\mathrm{Re} = 0.1$, 1, 10 and 100 is obtained with $(r_E, c, N_r) = (1200, 0.642, 129)$, $(600, 0.645, 129)$, $(600, 0.642, 257)$ and $(300, 0.642, 129)$, respectively. For $\mathrm{Re} = 10$, $N_r = 257$ is used with the first grid size $\Delta r = 0.01985$, because we want to minimize the effect of the truncation error on the long-time history force. When $N_r = 129$ is used for $\mathrm{Re} = 10$ under otherwise identical conditions, the decay behavior of the history force does not change. Thus, $N_r = 129$ is used for the other three values of Re. As will be discussed later, the small-time result computed separately with smaller grid and time-step sizes can be joined smoothly with the long-time result to give an accurate history force over a time span of 4–5 decades. For $\mathrm{Re} = 40$, $(r_E, c, N_r) = (100, 0.645, 129)$ is used with $N_\theta = 129$ and the computation is carried to $t = 80$ from which the long-time behavior of the history force can be inferred.

The second-order spatial derivatives are expressed using central difference. The convection term is discretized using a second-order upwind scheme in a conservative form (Mei & Plotkin 1986). This eliminates the numerical oscillation in space and enhances the convergence for higher values of Re over the central-difference scheme. The time derivative is evaluated using a backward Euler scheme which is implicit and first-order accurate in time. The numerical boundary condition for the vorticity is evaluated from the stream function on the grid points near the wall using a second-order-accurate expression derived by Briley (1971). The solutions for ψ and g are obtained in an iterative manner using a tridiagonal solver in the normal direction with a relaxation factor for the wall vorticity update.

2.2.3. Time-step size and iteration procedure

To capture the rapid transient accurately, the time-step size in the initial computation is $\Delta t = 0.001$ except for $\mathrm{Re} = 100$. It is gradually increased to 0.002, 0.005, 0.01 or larger, depending

on Re. At each time step, a large number of iterations (typically between 160–200) is executed. Although not optimized, the computation yields consistent and accurate results for the unsteady drag. Numerical solutions are accepted to be grid independent when the unsteady drag using $N_r = 65$ and 129 agree within 1% for the history force at $t \sim 0.1$ under otherwise identical conditions. It is found that the numerical result for the unsteady drag is repeatable using different values of time-step size on the same grid. For Re = 100, details are given in section 3.1.

To obtain accurate long-time behavior of the history force, separate runs are carried out with $\Delta t = 0.1$ between $t = 0.1$ to 50 for Re = 0.1, 1 and 10. After $t = 50$, computations are continued with $\Delta t = 0.25$ or 0.5 to save on computational effort. For Re = 100, $\Delta t = 0.1$ is used for $t = 0.1$ to 250. The results to be presented later are obtained simply by joining the short-time (typically for $t < 0.1$ to 0.5) and the long-time results. Such a combination with different values of r_E, N_r, c and Δt can be quite smooth in the overlapping time intervals.

It is noticed that $\psi(t, r, \theta) \sim \frac{1}{2} r^2 \sin^2\theta$ as $r \to \infty$. For $r_E = 1200$, the stream function at $t = 10$ ranges from 0.00485 (first grid away from the wall) to 720,000 at $r = r_E$. Such a large variation in ψ, by a factor of 10^8, causes numerical inaccuracy in solving [25]. To minimize the computational error, the stream function $\psi(t, r, \theta)$ is separated into two parts: a steady potential part that accounts for the large variation in ψ and a viscous unsteady part to be determined:

$$\psi(t, r, \theta) = \psi_p(r, \theta) + \psi_v(t, r, \theta) \tag{32}$$

and

$$\psi_p(r, \theta) = \tfrac{1}{2}(r^2 - r^{-1})\sin^2\theta. \tag{33}$$

The equation for $\psi_v(t, r, \theta)$ is

$$\mathscr{D}^2 \psi_v = g. \tag{34}$$

The boundary conditions for ψ_v in the r-direction are:

$$\psi_v = 0 \quad \text{at } r = 1; \qquad \frac{\partial \psi_v}{\partial r} = 0 \quad \text{at } r = r_E. \tag{35}$$

The condition for ψ_v at $r = r_E$ is better than setting $\psi_v = 0$ because it allows for the incorporation of the displacement effect of the viscous flow. Double precision is used for all the computations.

The procedure for evaluating the drag, which consists of a pressure component and a viscous component, is given in Mei *et al.* (1991). The history-force kernel $K(t')$ for both $U_1 = 0$ and $U_1 > 0$ can be determined from [13b].

3. RESULTS AND DISCUSSIONS

3.1. Accuracy Test

For a step change in the free-stream velocity from $U_1 = 0$ to $U_2 = 1$, with finite $\mathrm{Re} = 2aU_2/\nu$, accurate numerical solutions were obtained previously by Dennis & Walker (1972) using boundary-layer coordinates in the initial stage and switching to physical space at later times. The initial condition was based on the unsteady boundary layer solution which is accurate for small time. Figure 1(a) compares the computed drag (normalized by the Stokes drag $Ds = 6\pi\mu U_2 a$), $D(t)/Ds$, with that of Dennis & Walker (1972) for Re = 40 and 100. Excellent agreement can be observed.

Figure 1(b) compares the normalized unsteady drag for Re = 10 and small time using three different grids, $(r_E, c, N_r) = (50, 0.655, 65)$, $(90, 0.645, 65)$ and $(90, 0.645, 129)$, with $\Delta t = 0.001$. At small time, the vorticity is confined to the Stokes layer and the size of the physical domain, r_E, is not important. It can be seen clearly that the solutions are independent of the grid size for $t > 0.02$. For Re = 40 and 100, grid-independent solutions were obtained (not shown here) between $N_r = 65$ and 129 at $t \sim 0.06$. From figure 2(b) it can be seen that a coarser grid leads to stronger oscillation at the beginning of the computation than a finer grid. This oscillation was due to the fact that the finite grid size cannot resolve the initially very thin Stokes layer. It dies out fast and does not affect the solution at later time when the unsteady boundary layer grows and the grid

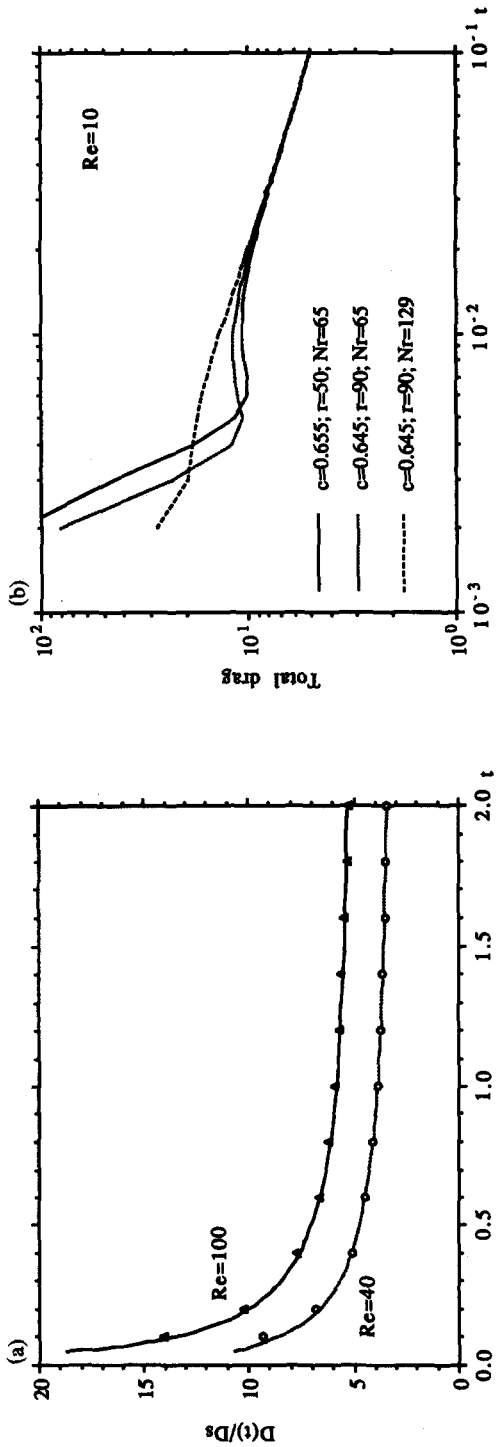

Figure 1. (a) Comparison of the drag coefficient $D(t)/Ds$ at Re = 40 and 100. Symbols—Dennis & Walker (1972); curves—present work. (b) Effect of the grid arrangement on the accuracy of the computed drag at Re = 10.

Figure 2. Comparison of the history force on a sphere due to a step change in the free-stream velocity from 0 to 1 based on various predictions: (a) log–log plot; (b) semi-log plot. Re = 0.1.

resolution becomes sufficient. For this reason, the flow fields for all Re at small times are obtained using $N_r = 129$. For $\mathrm{Re} = 40$, $(r_E, c, N_r) = (50, 0.645, 129)$ are used for $t < 0.1$ with $\Delta t = 0.001$. Another solution is obtained using $(r_E, c, N_r) = (50, 0.645, 65)$ for $0.001 \leqslant t < 10$ to minimize the amount of computational effort. The long-time history force is obtained using $(r_E, c, N_r) = (100, 0.645, 129)$ and $N_\theta = 129$ for $t < 80$. It is found that in the overlapping regions, these solutions agree very well with each other and can be joined very smoothly. For $\mathrm{Re} = 100$, $(r_E, c, N_r) = (25, 0.64, 129)$ are used for the initial calculation, $t \leqslant 0.1$, with $\Delta t = 0.00025$ to resolve the very thin unsteady boundary layer. A second run with $(r_E, c, N_r) = (50, 0.645, 129)$ was carried out for $0.001 < t < 10$ with $\Delta t = 0.001$. For this grid, the physical domain is large enough for $t < 10$. A third solution was obtained using $(r_E, c, N_r) = (50, 0.645, 65)$. For $t > 0.06$, the results of $(r_E, c, N_r) = (50, 0.645, 129)$ and $(r_E, c, N_r) = (50, 0.645, 65)$ agree very well, which indicates that: (i) the solution for $\mathrm{Re} = 100$ is grid independent at small and intermediate times; and (ii) the solutions for the history force obtained on different grids with different time-step size and physical-domain size can be joined smoothly. As mentioned earlier, the history force for $t \sim 100$ or larger is obtained (by starting from $t = 0.1$) on a much larger physical domain.

3.2. *Decay of the History Force*

3.2.1. *Impulsively started motion from $U_1 = 0$ to $U_2 = 1$*

For an impulsively started motion in the free-stream velocity from $U = U_1 = 0$ to $U = U_2 = 1$ with $\mathrm{Re} \ll 1$, an analytical result based on matched asymptotic expansion for the unsteady drag was given by Sano (1981) as

$$\frac{D(t)}{Ds} = 1 + \frac{1}{\sqrt{\frac{\pi t}{\mathrm{Re}'}}} + \tfrac{3}{8}\mathrm{Re}'\left[\left(1 + \frac{4}{T^2}\right)\mathrm{erf}(\tfrac{1}{2}\sqrt{T}) + \frac{2}{\sqrt{\pi T}}\left(1 - \frac{2}{T}\right)\mathrm{e}^{-T/4} - \frac{8}{3}\frac{1}{\sqrt{\pi T}}\right] + \tfrac{1}{3}\delta(t) + O(\mathrm{Re}'^2 \log \mathrm{Re}'), \quad [36]$$

where $\mathrm{Re}' = \mathrm{Re}/2$, $T = \mathrm{Re}'\, t$ and the delta function $\delta(t)$ results from the added-mass force and the force due to the free-stream acceleration at $t = 0$. It is noted that the steady-state drag D_∞ is

$$\frac{D_\infty}{Ds} = \lim_{t\to\infty} \frac{D(t)}{6\pi\mu U_2 a} = 1 + \tfrac{3}{8}\mathrm{Re}' + O(\mathrm{Re}^2 \log \mathrm{Re}). \quad [37]$$

Thus, the history-force kernel can be deduced from the above as

$$K_{\mathrm{Sano}}(t) = \frac{1}{\sqrt{\frac{\pi t}{\mathrm{Re}'}}} + \tfrac{3}{8}\mathrm{Re}'\left[\left(1 + \frac{4}{T^2}\right)\mathrm{erf}(\tfrac{1}{2}\sqrt{T}) + \frac{2}{\sqrt{\pi T}}\left(1 - \frac{2}{T}\right)\mathrm{e}^{-T/4} - \frac{8}{3}\frac{1}{\sqrt{\pi T}}\right] - \tfrac{3}{8}\mathrm{Re}'. \quad [38]$$

In the limit of large t, $K_{\mathrm{Sano}}(t) \sim 3/(\mathrm{Re}\, t^2)$.

Figure 2(a) compares five different predictions for the history force in log–log coordinates for $\mathrm{Re} = 0.1$. They are: Basset's solution (1888); Sano's (1981) solution; the finite-difference solution outlined above, which is considered to be the exact solution; Mei & Adrian's (1992) expression given by [7a, b]; and Odar & Hamilton's (1964) expression. Based on Odar & Hamilton (1964), the history force in the present case with an infinite acceleration at $t = 0$ is the original Basset force multiplied by a factor of 0.48. At small time, say $t < 1$, the decay of $K(t)$ is clearly $t^{-1/2}$. It can be seen that all predictions agree well for $t < 1$, except for that given by Odar & Hamilton (1964). It was pointed out in Mei (1993) that Odar & Hamilton's (1964) empirical expression does not approach the limiting value of the history force for $t \ll 1$ given by Basset (1888). Therefore, the predictions using Odar & Hamilton's expression for other Re will not be presented. The Basset solution for $t > 1$ decays too slowly and it is not recommended, in general, for the evaluation of the history force at large time. Of course, as $\mathrm{Re} \to 0$, the validity of the Basset solution, $K(t) \sim t^{-1/2}$, will be extended to larger time. However, if one fixes the Re first, no matter how small, there will be a time beyond which the Basset solution is not valid. Nevertheless, in practical cases, the Basset

solution can be used for very small Re for small and intermediate time which could be even larger than the physical time scale of interest.

At intermediate time, $t < 200$, Sano's (1981) analytical result agrees well with that of the finite-difference solution obtained using $(r_E, c, N_r) = (1200, 0.642, 129)$. However, for $t > 200$, the finite-difference solution clearly shows a decay faster than t^{-2}. In fact, the decay is even not algebraic anymore. As shown in figure 2(b), the history force actually decays exponentially for $t > 260$, as

$$K(t) \sim 0.001783\, e^{-0.00625t}, \quad \text{for } t > 260, \tag{39}$$

as opposed to $K_{Sano}(t) \sim 3/(\mathrm{Re}\, t^2)$ for large t. Note that the physical domain is $r \leqslant r_E = 1200$, which is still much larger than the distance traveled by the disturbance originating from the sphere at $t \sim 260$. The stored flow fields at $t = 200$ and 600 do indicate that in the wake region the vorticity has a "rapid" drop-off (seen on the log scale) near $x \sim 200$ and 600, respectively. In the remaining grids between $x \sim 600$ and $x = 1200$, the vorticity is zero for $t = 600$. Thus, the numerical boundary condition at $r = r_E$ given by [35] should not have any effect on the history force for $t < 600$. The simple exponential decay, [39], continues to hold up to $t = 800$ when the computation is ended.

The expression given by Mei & Adrian (1992) underestimates the history force for $t < 800$ for $\mathrm{Re} = 0.1$. By comparing with the present numerical solution, the analytical approximation for $K(t)$ given by [7a] does not have an exponential decay at large time. Thus, it cannot be qualitatively accurate for very large time. It can be seen that Sano's (1981) expression, Mei & Adrian's (1992) expression and the numerical result all exhibit a t^{-2} decay in the intermediate time which is an important feature. From a practical point of view, since the largest difference in $K(t)$ between [7a,b] and [38] for $\mathrm{Re} = 0.1$ is 0.015 at $t = 3$ and the difference exceeds 0.01 only for $0.5 < t < 16$, [7a] does give a quite reliable estimate for $K(t)$ at $\mathrm{Re} = 0.1$ for flows with such strongly singular acceleration.

Figure 3(a) shows a similar comparison at $\mathrm{Re} = 1$ in log–log coordinates. Very similar behavior is observed. A t^{-n} decay ($n \sim 2$ or slightly larger) can be observed for $20 < t < 160$ from the finite-difference solution. The numerical result also exhibits an exponential decay of the history force after $t \sim 160$, as shown in figure 3(b). Again, the size of the physical domain and the grid size should not affect the qualitative behavior of the history force for $t < 400$ because $r_E = 600$. The largest absolute difference between the prediction using [7a, b] and the finite-difference solution is 0.12 at $t = 0.4$, with a relative error of 7%.

Figure 4(a) compares the history force for $\mathrm{Re} = 10$ predicted using Sano's expression [34], that using the expression of Mei & Adrian [7a, b] and the finite-difference solution with $(r_E, c, N_r) = (600, 0.642, 257)$. The initial decay of the history force is again $t^{-1/2}$. A t^{-n} decay ($n \sim 2$ or a little larger) is seen for $40 < t < 160$. As shown clearly in figure 4(b), the history force starts to decay exponentially at $t \sim 160$. It is noted that Sano's solution is supposedly valid for small Re and is not expected to give close agreement with the finite-difference result for $\mathrm{Re} > 1$. Comparing it with the numerical result, it seems that Sano's result is still quite good for $\mathrm{Re} = 10$ for small and intermediate time. Since Mei & Adrian's expression takes the effect of finite Re into consideration, it is expected to be approximately valid for finite Re. Figure 4 confirms this observation for small and intermediate time. Figure 5 shows the computed and predicted history force for small and intermediate time for $\mathrm{Re} = 40$ using $N_\theta = 129$ and $(r_E, c, N_r) = (100, 0.645, 129)$ for the intermediate time computation. It is clear from figure 5(a) that $K(t)$ decays faster than t^{-2} after $t \sim 15$ and the decay is not algebraic. The exponential decay can be seen in figure 5(b) for $t > 40$. The agreement between the analytical prediction and the numerical results can be considered quite good from a practical point of view.

At $\mathrm{Re} = 100$, a "large" Reynolds number case, the history force behavior is more complex. Figure 6(a) indicates that for $t < 0.03$, $K(t)$ decays as $t^{-1/2}$, a classical result of Basset (1888). It can be noticed that $K(t)$ decays at a slower rate near $t \sim 1.3$ because the pressure force actually increases slightly between $t = 1.3$ to 2.8, while the frictional force is continuously decreasing. This behavior was independent of the grid arrangement and time-step size. It is related to the expansion of the separation bubble in the rear of the sphere. A rough curve fit of $K(t) \sim t^{-0.82}$ may be used to describe the decay of $K(t)$ approximately for $0.06 < t < 6$. For $6 < t < 20$, the history force decays as $K(t) \sim 0.754 \exp(-0.17t)$. As seen from figure 6(b), a much slower exponential decay

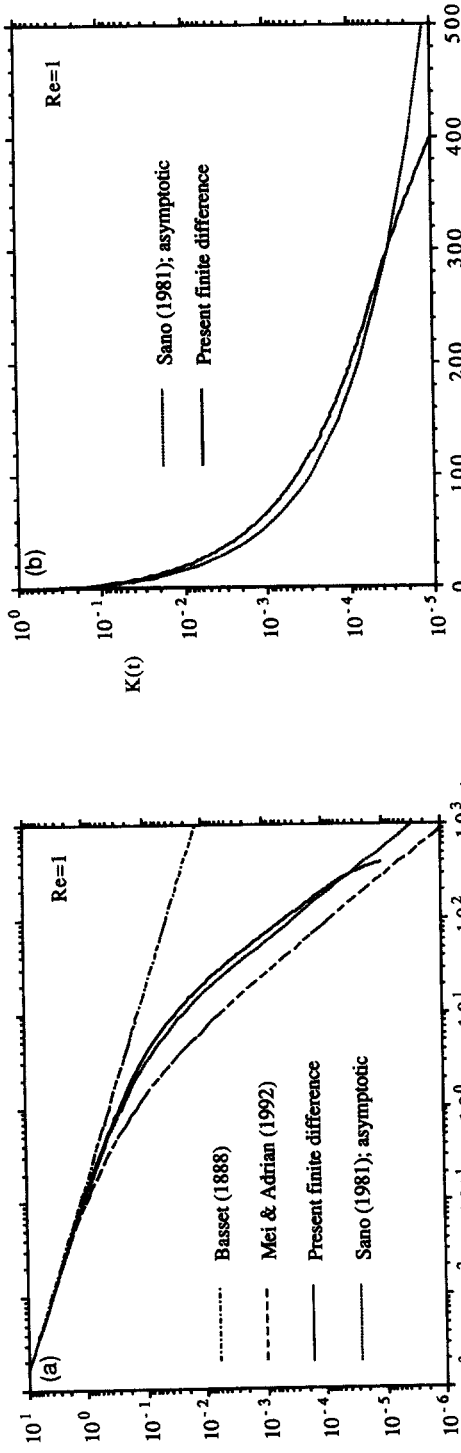

Figure 3. Comparison of the history force on a sphere due to a step change in the free-stream velocity from 0 to 1 based on various predictions: (a) log–log plot; (b) semi-log plot. Re = 1.

Figure 4. Comparison of the history force on a sphere due to a step change in the free-stream velocity from 0 to 1 based on various predictions: (a) log–log plot; (b) semi-log plot. Re = 10.

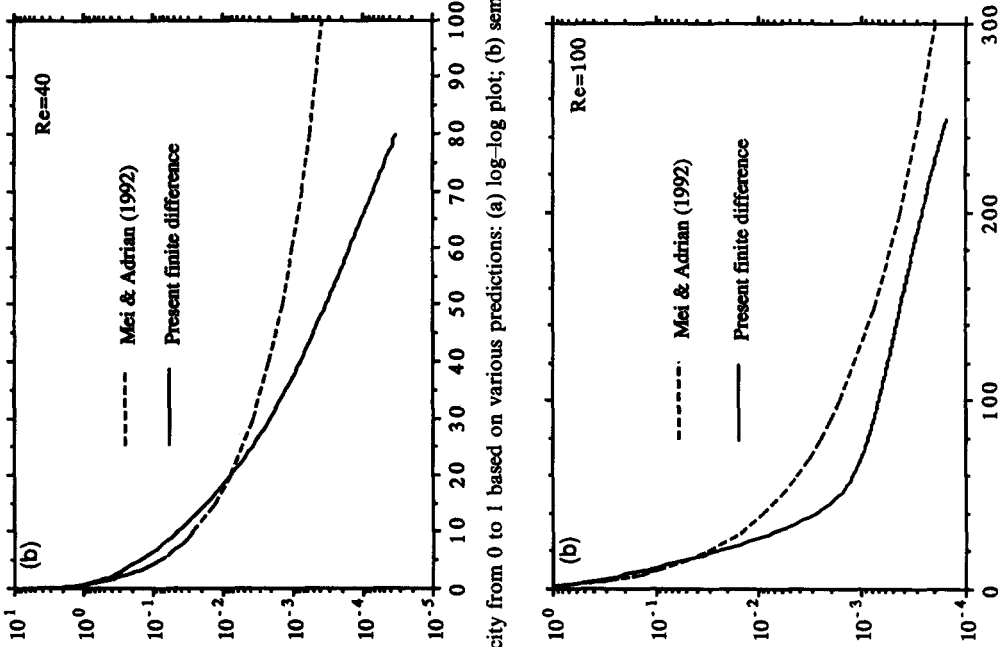

Figure 5. Comparison of the history force on a sphere due to a step change in the free-stream velocity from 0 to 1 based on various predictions: (a) log–log plot; (b) semi-log plot. Re = 40.

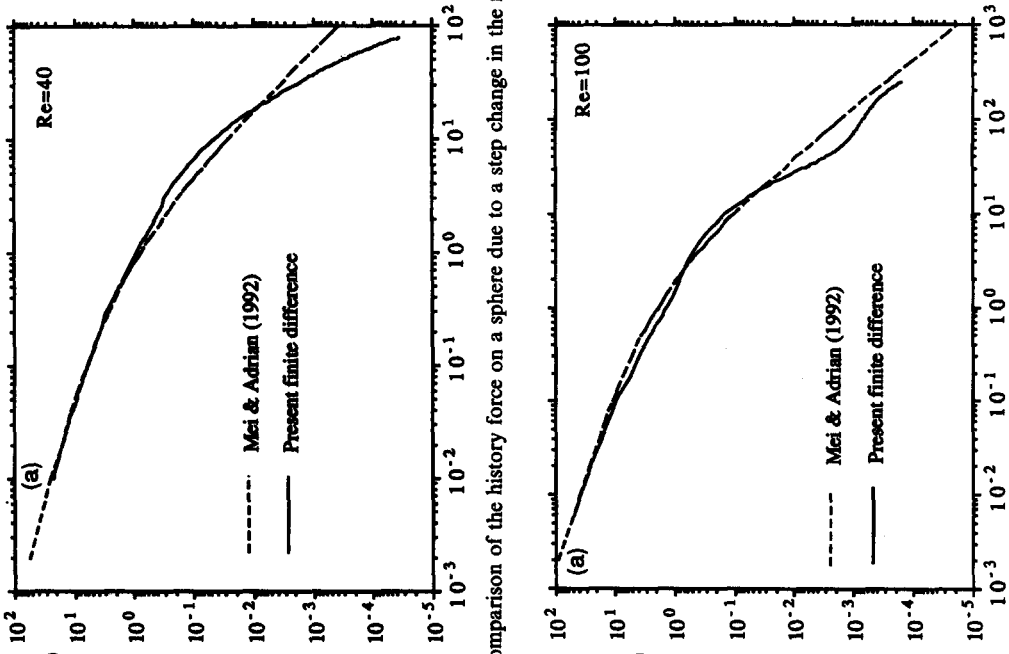

Figure 6. Comparison of the history force on a sphere due to a step change in the free-stream velocity from 0 to 1 based on various predictions: (a) log–log plot; (b) semi-log plot. Re = 100.

is established as $K(t) \sim 0.0184 \exp(-0.00985t)$ for $t > 80$. A transition region between these two exponential decays exists for $20 < t < 80$. From a practical point of view, the prediction using Mei & Adrian's (1992) expression would still give a reliable estimate at Re = 100 over a large range of time, although exponential decay does not exist in the analytical prediction.

3.2.2. A step change from $U_1 (0 < U_1 < 1)$ to $U_2 = 1$

For a step change from $U = U_1$ to $U = U_2$ at finite Re, no known analyses exist to evaluate the unsteady force for all times. The approximate expression of Mei & Adrian, [7a, b], would be good only if

$$\alpha = \frac{|U_2 - U_1|}{U_2} \ll 1. \qquad [40]$$

Attention is paid to this case with $U_1 > 0$, because the effect of an existing steady velocity field at $\mathrm{Re}_1 = U_1 2a/\nu$ on the history force is not clear.

Figure 7(a) compares the history forces predicted using Basset's (1888) solution, Mei & Adrian's expression and that computed using the finite-difference method for $(\alpha, \mathrm{Re}) = (0.2, 1)$. The prediction using Odar & Hamilton's expression is not shown because it is even not correct at very small t. The numerical results presented here are based on the solutions obtained with $(r_E, c, N_r) = (600, 0.645, 129)$. As discussed previously, the numerical solution for the unsteady drag in the initial transient is inaccurate, since the finite grid size cannot resolve the thin boundary layer near $t \sim 0$ caused by the sudden change in the vorticity. After a short period of the initial transient, the analytical prediction agrees well with the numerical solution for both small and intermediate time. A decay that is faster than t^{-2} is observed for $7 < t < 200$ in figure 7(a). The agreement between the analytical prediction and the numerical results is better for $\alpha = 0.2$ than that for $\alpha = 1$ for $t < 200$. Figure 7(b) shows that from $t > 160$, the history force decays exponentially. Furthermore, the decay rate is nearly the same as in the case of $\alpha = 1$, since the two curves are parallel to each other in the semi-log coordinates.

Figure 8(a) shows the history force for Re = 10 with $\alpha = 0.2$ in log–log coordinates. The steady flow field is obtained first for Re = 8 with $(r_E, c, N_r) = (600, 0.642, 257)$. A step change is imposed in the free-stream velocity, resulting in Re = 10 based on the new free-stream velocity. The history force with $\alpha = 0.2$ is qualitatively similar to that at Re = 10 with $\alpha = 1$ for $t < 600$. The exponential decay at long time can be seen in figure 8(b). It may be noticed that a decay that is slightly faster than a simple exponential decay exists for $t > 500$. However, since the magnitude of the history force at $t \sim 500$ is so small, the faster decay is of little practical concern at such large time. It is also seen that the analytical prediction using [7a, b] is satisfactory in comparison with the numerical result.

3.3. Discussion

From the above comparisons for both $U_1 = 0$ and $U_1 > 0$, it can be concluded that the history-force kernel at finite Re has the following gross features: (i) $K(t) \sim t^{-1/2}$ for small time; (ii) $K(t) \sim t^{-n}$ $(n \geqslant 2)$ for intermediate time; and (iii) $K(t) \sim \mathrm{e}^{-\beta t}$ at very large time. For small time, an $O(1)$ error is expected for $K(t)$ because of the $O(1)$ error in representing the quasi-steady force by [3]. However, this error is small and not noticeable because $K(t) \sim t^{-1/2}$. It is seen that the long-time exponential decay is observed in both the impulsively started motion and flows with a step change in the free-stream velocity over an established steady flow. The existing steady flow field does not affect the qualitative feature of the history force. This has the following implication. For a particle in a turbulent fluid, any disturbance, say due to a strong turbulent eddy or due to a shock wave, introduced at *any instant* of the motion will eventually decay exponentially.

It is interesting to note that Sano's (1981) asymptotic solution does not predict an exponential decay for the history force, while the present solution clearly shows the existence of such an exponential decay at large time. Careful examination of figure 2(a) indicates that the difference between his asymptotic solution and the present "exact" numerical solution is $< 10^{-4}$ at Re = 0.1. It is possible that the difference results from the high-order nonlinear interaction that is picked up in the present numerical solution but is neglected in the asymptotic analysis which uses linearized Navier–Stokes equations in the Stokes and the Oseen regions.

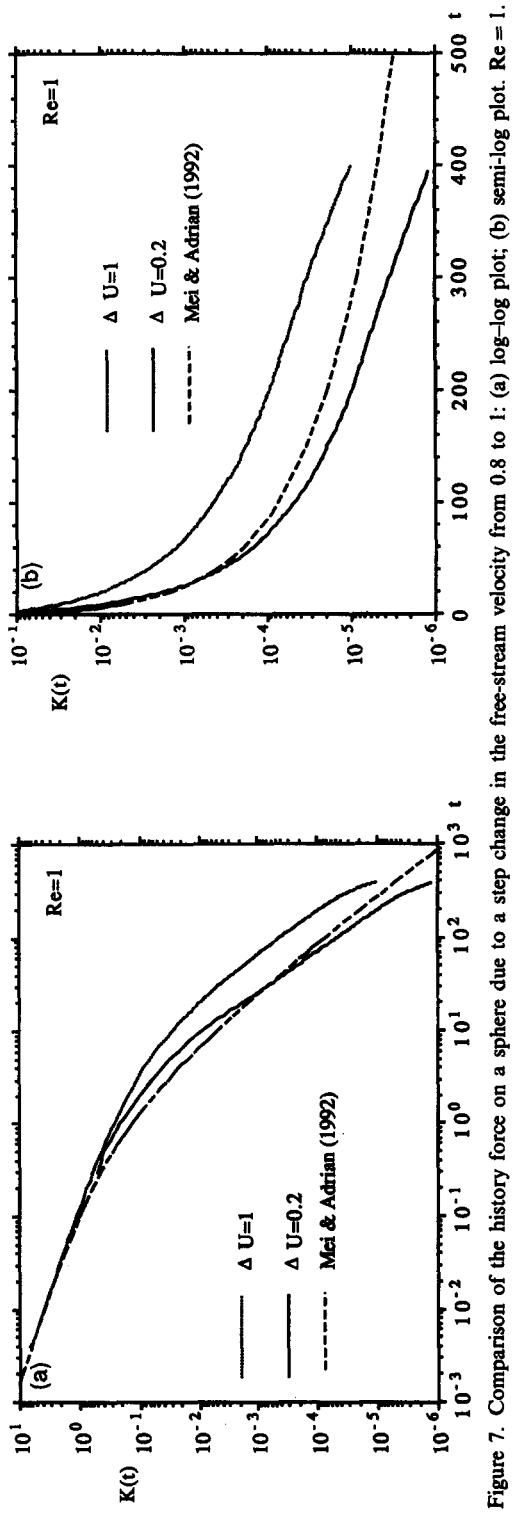

Figure 7. Comparison of the history force on a sphere due to a step change in the free-stream velocity from 0.8 to 1: (a) log–log plot; (b) semi-log plot. Re = 1.

Figure 8. Comparison of the history force on a sphere due to a step change in the free-stream velocity from 0.8 to 1: (a) log–log plot; (b) semi-log plot. Re = 10.

From the above comparisons, [7a, b] give a reliable estimate for the history force even for unsteady flows with a strongly singular acceleration. Combined with the studies reported in Mei *et al.* (1991) and Mei (1993), it seems that the expression for the history-force kernel given by Mei & Adrian (1992) can be used to evaluate the history force for small and intermediate time for different kinds of unsteady flows. Equations [7a, b] should be useful for practical applications. Basset's (1888) expression is not recommended to evaluate the history force for order one or larger values of Re at large time. The expressions of Odar & Hamilton (1964) grossly misrepresent the history force and the added-mass force in the case of a sudden change in the velocity.

With [7a, b] tested satisfactorily for flows with sudden changes in the free-stream velocity, an attempt was made, using [3]–[8] in a two-dimensional form, to predict the droplet trajectory as in the experimental investigation of Temkin & Kim (1980). In the experiments of Temkin & Kim (1980), the motions of the droplets are two-dimensional because the droplets were injected into a horizontal shock tube with significant vertical velocity. It was found that the history force in the form of [7a, b] contributes very little to the total force in [3] and causes no noticeable change in the droplet velocity. If the Basset (1888) solution with $t^{-1/2}$ decay is used in place of [7a, b], there is a noticeable change in the droplet velocity because the decay is too slow. However, it is clearly demonstrated in this investigation that the Basset solution is not correct and should not be used in this case. A complete neglect of F_H, F_{AM} and F_{FS} yields almost identical results because the density ratio of the droplet to the air is very large and the history force decays very fast according to [7a, b]. Thus, we cannot expect to use the experimental data of Temkin & Kim (1980) and Temkin & Mehta (1982) to verify the proposed expression for the history force. It can also be said, based on the present study, that the history force and the added-mass force should not be important factors in the droplet motion investigated by Temkin & Kim (1980). Similar conclusions regarding the effect of the added-mass force and the history force were reached by Linteris *et al.* (1991) in their investigation of the motions of droplets entering a horizontal air jet from above with a vertical velocity equal to the terminal velocity of the droplet. Using [3]–[8], good agreements for the droplet trajectory and velocity were achieved between the measurement (Temkin & Kim 1980) and the present prediction only for cases with large fluid horizontal velocity (in comparison with the vertical injection velocity), thus having relatively smaller wake effects but larger Re and We (Weber number). However, these data were considered by Temkin & Kim (1980) as having too much uncertainty due to the droplet deformation and shape oscillation [maximum We close to or exceeding 0.15, a marginal value defined by Temkin & Kim (1980)]. Thus, the agreement may be just fortuitous and the result is not reported here. The fact that Temkin & Kim (1980) deduced a larger drag coefficient from most of the droplet trajectories with decelerating relative velocity (between the droplet and the fluid) cannot be explained by the present particle dynamic equations [3]–[8], because the dynamics is developed for single particles; while in Temkin & Kim (1980) the wake of the droplet string may have complicated effects at finite Re.

4. CONCLUSIONS

Accurate finite-difference solutions are obtained for unsteady flows over a stationary sphere due to sudden changes in the free-stream velocity for Re ranging from 0.1 to 100 over a large range of time. An exponential decay of the history force is observed for large time for small and large Re. The expression for unsteady drag proposed by Mei & Adrian (1992) is assessed. The expression gives accurate predictions for the history force at small time for all Re investigated. For intermediate time, the analytical prediction can be considered satisfactory.

Acknowledgements—The author thanks Professor J. F. Klausner for his input during the preparation of the manuscript. Professor C. J. Lawrence's review helped improve the paper and was greatly appreciated.

REFERENCES

BASSET, A. B. 1888 *A Treatise On Hydrodynamics*, Vol. 2. Dover, London.

BENTWICH, M. & MILOH, T. 1978 The unsteady matched Stokes–Oseen solution for the flow past a sphere. *J. Fluid Mech.* **88**, 17–32.

BRILEY, M. R. 1971 A numerical study of laminar separation bubbles using the Navier–Stokes equations. *J. Fluid Mech.* **47,** 713–736.

CLIFT, R., GRACE, J. R. & WEBER, M. E. 1978 *Bubbles, Drops and Particles.* Academic Press, New York.

DENNIS, S. C. R. & WALKER, J. D. A. 1972 Numerical solutions for time-dependent flow past an impulsively started sphere. *Phys. Fluids* **15,** 517–525.

KARANFILIAN, S. K. & KOTAS, T. J. 1978 Drag on a sphere in unsteady motion in a liquid at rest. *J. Fluid Mech.* **87,** 88–96.

LINTERIS, G. T., LIBBY, P. A. & WILLIAMS, F. A. 1991 Droplet dynamics in a nonuniform field. *Combust. Sci. Technol.* **80,** 319–335.

MAXEY, M. R. & RILEY, J. J. 1983 Equation of motion for a small rigid sphere in a nonuniform flow. *Phys. Fluids* **26,** 863–889.

MEI, R. 1990 Particle dispersion in isotropic turbulence and unsteady particle dynamics at finite Reynolds number. Ph.D. Thesis, Univ. of Illinois at Urbana-Champaign, IL.

MEI, R. 1993 Flow due to an oscillating sphere and an expression for unsteady drag on the sphere at finite Reynolds number. *J. Fluid Mech.* In press.

MEI, R. & PLOTKIN, A. 1986 Navier–Stokes solution for some laminar incompressible flows with separation in forward facing step geometries. *AIAA Jl* **24,** 1106–1111.

MEI, R & ADRIAN, R. J. 1992 Flow past a sphere with an oscillation in the free-stream velocity and unsteady drag at finite Reynolds number. *J. Fluid Mech.* **237,** 323–341.

MEI, R., LAWRENCE, C. J. & ADRIAN, R. J. 1991 Unsteady drag on a sphere at finite Reynolds number with small fluctuations in the free-stream velocity. *J. Fluid Mech.* **233,** 613–628.

MOORMAN, R. W. 1955 Motion of a spherical particle in the accelerated portion of free fall. Ph.D. Thesis, Univ. of Iowa, Ames, IA.

ODAR, F. 1966 Verification of the proposed equation for calculation of the forces on a sphere accelerating in a viscous fluid. *J. Fluid Mech.* **25,** 591–592.

ODAR, F. & HAMILTON, W. S. 1964 Forces on a sphere accelerating in a viscous fluid. *J. Fluid Mech.* **18,** 302–314.

RIVERO, M., MAGNAUDET, J. & FARBE, J. 1991 Quelques résultats nouveaux concernant les forces exercées sur une inclusion sphérique par ecoulement accéléré (New results on the forces exerted on a spherical body by an accelerated flow). *C. R. Acad. Sci. Paris Série II* **312,** 1499–1506.

SANO, T. 1981 Unsteady flow past a sphere at low Reynolds number. *J. Fluid Mech.* **112,** 433–441.

SCHÖNEBORN, P.-R. 1975 The interaction between a single particle and oscillating fluid. *Int. J. Multiphase Flow* **2,** 307–317.

STOKES, G. G. 1851 On the effect of internal friction of fluids on the motion of pendulum. *Trans. Camb. Phil. Soc.* **9,** 8. Reprinted in *Mathematics and Physics Papers III.* Cambridge University Press, U.K. (1922).

TEMKIN, S. & KIM, S. S. 1980 Droplet motion induced by weak shock waves. *J. Fluid Mech.* **96,** 133–157.

TEMKIN, S. & MEHTA, H. K. 1982 Droplet drag in an accelerating and decelerating flow. *J. Fluid Mech.* **116,** 297–313.

TSUJI, Y., KATO, N. & TANAKA, T. 1991 Experiments on the unsteady drag and wake of a sphere at high Reynolds numbers. *Int. J. Multiphase Flow* **17,** 343–354.